The First Generation NIMROD Production Code

Carl R. Sovinec
Los Alamos National Laboratory

and

The NIMROD Team

presented at the

Thirty-ninth Annual Meeting of the Division of Plasma Physics

November 17-21, 1997

Pittsburgh, Pennsylvania

Main Points

- The essential features of NIMROD are ready for attacking research problems associated with low-frequency MHD activity in fusion-relevant plasmas.

- NIMROD has been formulated to avoid accuracy constraints on the time step associated with compressional Alfven waves. It has been coded in a modular fashion for flexibility and ease of use. Parallel features have been incorporated from the beginning of code development.

- NIMROD is presently being benchmarked against ideal MHD instability results from GATO and resistive MHD instability results from DEBS. We are also comparing nonlinear saturation amplitudes between NIMROD and DEBS.

- Research simulations are underway! An RFP simulation in toroidal geometry has been started, and plans for addressing external modes with a vacuum region outside the separatrix are being developed.

Outline

I. Introduction

   A. List of active participants
   B. Code and project description
   C. Project goals

II. Development status

   A. Physics kernel
   B. Linear solver
   C. Preprocessing
   D. Postprocessing
   E. Graphical user interface

III. Validation program

   A. Linear waves
   B. Ideal MHD instabilities
   C. Resistive MHD instabilities
   D. Nonlinear results

IV. Plans for completing the first production version

V. Intermediate-term plans

VI. Summary

Introduction

List of Active Participants

Ming Chu	GA
Sergei Galkin	KIAM
Tom Gianakon	Cadarache
Alan Glasser	LANL
Harsh Karandikar	SAIC
Alice Koniges	LLNL
Scott Kruger	U-WI
Rick Nebel	LANL
Dan Laney	LLNL
Alexander Pletzer	ITER
Steve Plimpton	SNL
Nina Popova	MSU
Dalton Schnack	SAIC
Carl Sovinec	LANL
Alfonso Tarditi	SAIC
Alan Turnbull	GA

Code and Project Description

NIMROD is a suite of codes for solving the two-fluid system of equations as functions of three spatial dimensions and time, including all nonlinear effects. The spatial discretization uses a mix of quadrilateral and triangular finite elements over the poloidal plane and Fourier series in the toroidal direction. The grid is decomposed into blocks, which may be run on separate processors of a parallel computer. The temporal discretization avoids explicit time-step limitations associated with natural modes of the two-fluid equations.

Besides the physics kernel (NIMROD), the suite includes a grid-generator (FLUXGRID), a preprocessor (NIMSET), a postprocessor (NIMPLOT), and a graphical user interface (GUI).

Project Goals

The goal for the NIMROD code is to simulate low-frequency nonlinear behavior...

- nonlinear evolution of tearing modes
- resistive wall modes
- neoclassical modes

...in realistic experimental geometries...

- D3D
- ITER
- reversed-field pinches
- spheromaks
- etc.

...including plasma rotation and electron dynamics.

An additional goal of the project is explore whether or not managerial techniques such as integrated product development and quality function deployment can assist a multi-disciplinary team composed of members at diverse locations when developing a large-scale computational tool.

Development Status

Physics Kernel

The physical foundation of NIMROD lies in the two-fluid/ Maxwell system of equations.

Separate Electron and Ion Fluid Equations (quasineutral and no displacement current):

$$n_e \cong Z_e n_i \equiv n, \quad Z_e \equiv -\frac{q_i}{q_e}$$

$$\frac{\partial n}{\partial t} + \nabla \cdot n\mathbf{V}_e = 0$$

$$m_\alpha n_\alpha \left(\frac{\partial}{\partial t} + \mathbf{V}_\alpha \cdot \nabla \right) \mathbf{V}_\alpha = n_\alpha q_\alpha \left(\mathbf{E} + \mathbf{V}_\alpha \times \mathbf{B} \right) - \nabla p_\alpha - \nabla \cdot \Pi_\alpha - \eta n_\alpha q_\alpha \mathbf{J}$$

$$\frac{3}{2}\left(\frac{\partial}{\partial t} + \mathbf{V}_\alpha \cdot \nabla \right) p_\alpha = -\frac{5}{2} p_\alpha \nabla \cdot \mathbf{V}_\alpha - \nabla \cdot \mathbf{q}_\alpha - \Pi_\alpha : \nabla \mathbf{V}_\alpha + Q_\alpha$$

where α=i,e

Maxwell's:

$$\mu_0 \mathbf{J} = \nabla \times \mathbf{B}$$

$$\frac{\partial \mathbf{B}}{\partial t} = -\nabla \times \mathbf{E}$$

Linear combinations produce an equivalent Single-Fluid form:

$$\rho = n\left(m_e + \frac{m_i}{Z_e}\right)$$

$$\rho\left(\frac{\partial}{\partial t} + \mathbf{V}\cdot\nabla\right)\mathbf{V} = \mathbf{J}\times\mathbf{B} - \nabla p' - \nabla\cdot\Pi'$$

$$\mathbf{E} = -\mathbf{V}\times\mathbf{B} + \frac{1}{en}\frac{\left(1 - Z_e m_e/m_i\right)}{\left(1 + Z_e m_e/m_i\right)}\mathbf{J}\times\mathbf{B} + \eta\mathbf{J}$$
$$+ \frac{1}{\varepsilon_0\omega_p^2}\left[\frac{\partial\mathbf{J}}{\partial t} + \nabla\cdot(\mathbf{JV} + \mathbf{VJ}) + \sum_\alpha \frac{q_\alpha}{m_\alpha}\left(\nabla p'_\alpha + \nabla\cdot\Pi'_\alpha\right)\right]$$

where

$$\omega_p^2 = \sum_\alpha \frac{n_\alpha q_\alpha}{\varepsilon_0 m_\alpha} \ ,$$

$$p' = \sum_\alpha p_{©\alpha} \ , \quad \Pi' = \sum_\alpha \Pi_{©\alpha} \ ,$$

and primes indicate the center of mass reference frame,

$$p_{©\alpha} = p_\alpha + \frac{n_\alpha m_\alpha}{3}\left(\mathbf{V}_\alpha - \mathbf{V}\right)^2$$

$$\Pi_{©\alpha} = \Pi_\alpha + n_\alpha m_\alpha\left(\mathbf{V}_\alpha - \mathbf{V}\right)\left(\mathbf{V}_\alpha - \mathbf{V}\right) - \mathbf{I}\left(p'_\alpha - p_\alpha\right)$$

At present we are solving:

$$\rho \frac{\partial \mathbf{V}}{\partial t} = \mathbf{J} \times \mathbf{B} - \nabla p' + \nabla \cdot \nu \nabla \mathbf{V} - \rho \mathbf{V} \cdot \nabla \mathbf{V}$$

$$\frac{3}{2}\left(\frac{\partial}{\partial t} + \mathbf{V} \cdot \nabla \right) p' = -\frac{5}{2} p' \nabla \cdot \mathbf{V}$$

$$\mu_0 \mathbf{J} = \nabla \times \mathbf{B}$$

$$\frac{\partial \mathbf{B}}{\partial t} = -\nabla \times \mathbf{E}$$

with the generalized Ohm's law including as much as

$$\mathbf{E} = -\mathbf{V} \times \mathbf{B} + \frac{1}{en} \frac{\left(1 - Z_e m_e / m_i\right)}{\left(1 + Z_e m_e / m_i\right)} \mathbf{J} \times \mathbf{B} + \eta \mathbf{J} + \frac{1}{\varepsilon_0 \omega_p^2} \left(\frac{\partial \mathbf{J}}{\partial t} \right)$$

These equations contain the normal modes of our complete system, and our success with the present implementation bodes well for solving the complete system.

NIMROD represents functions of space with 2-D finite elements for the poloidal plane and Fourier series for the perpendicular direction (toroidal or periodic linear).

The poloidal plane is decomposed into an unstructured collection of blocks. This permits geometric flexibility and creates a natural decomposition for running on parallel machines, where MPI is used for communication between processors.

NIMROD Grid

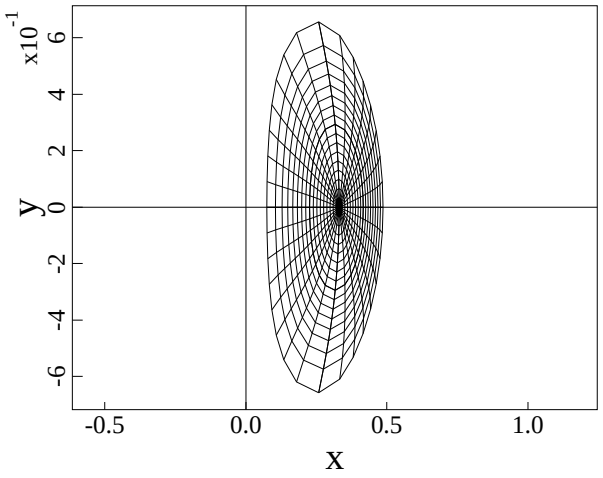

9-block Decomposition

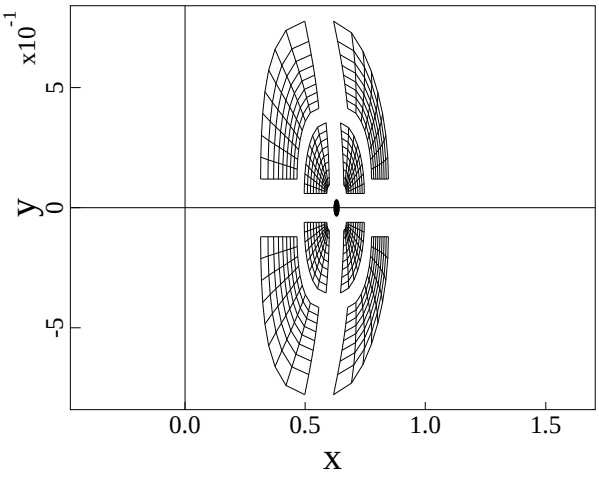

Central Block

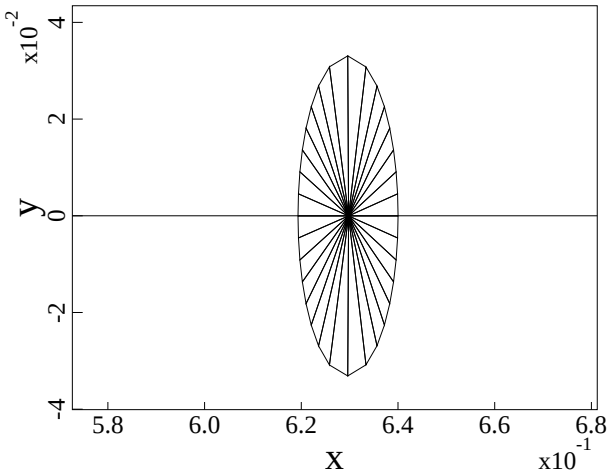

The blocks containing triangles are themselves unstructured and may be used for complex boundary shapes or for singular points in the grid. [However, we typically use degenerate rectangles at the O-point of the grid.]

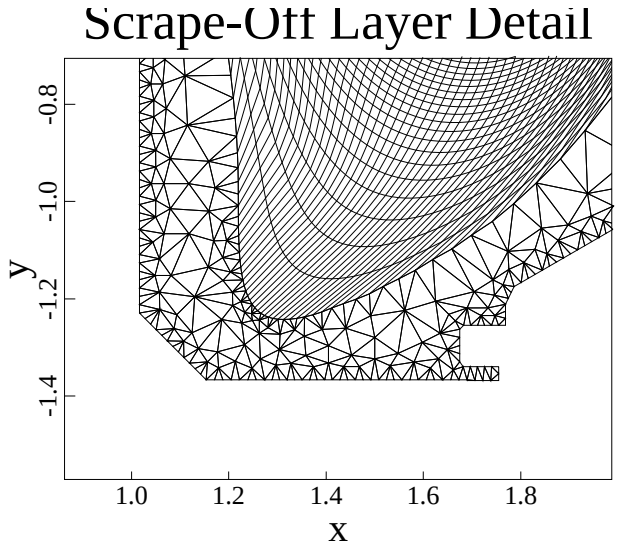

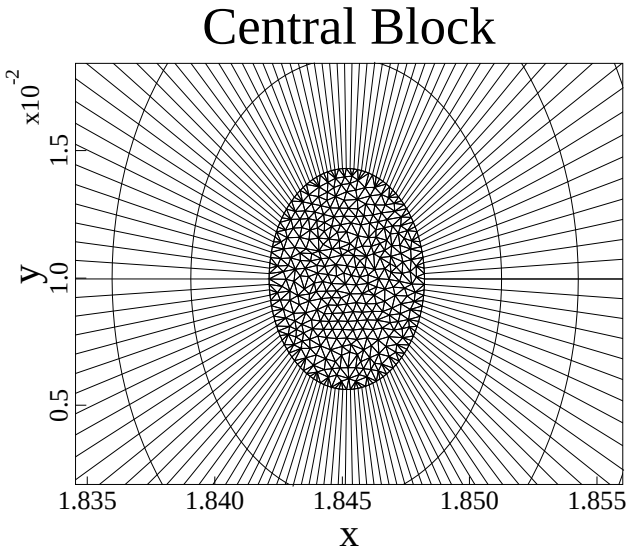

Functions of space have different basis functions according to the element shape:

- Quadrilaterals use bilinear basis functions for dependent variables.

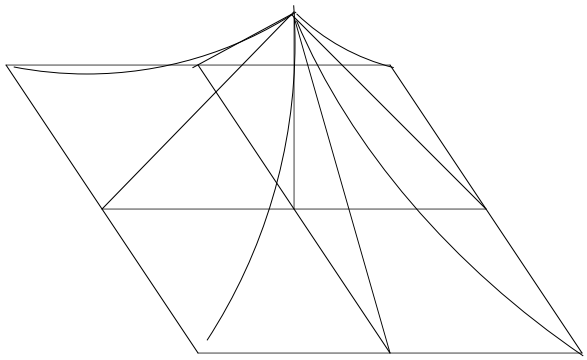

The grid and equilibrium quantities (separated from the perturbed quantities) are treated with bicubic splines.

- Triangles use linear basis functions for all functions.

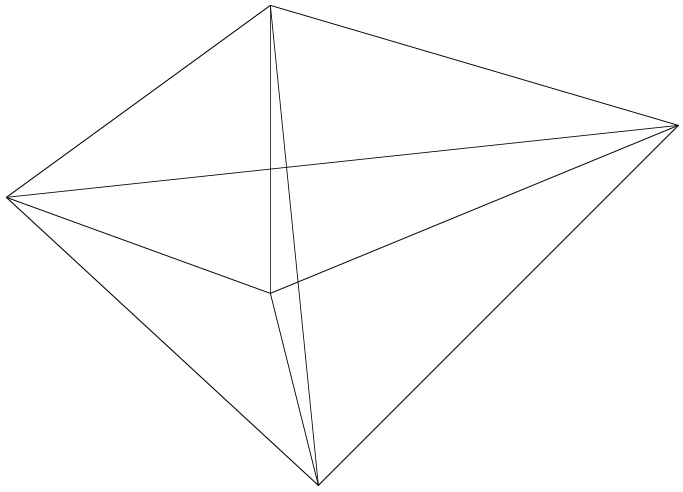

The NIMROD kernel is written in a highly modular fashion. The integrand routine for each equation is coded separately from the integration procedures, which are generic to each block type:

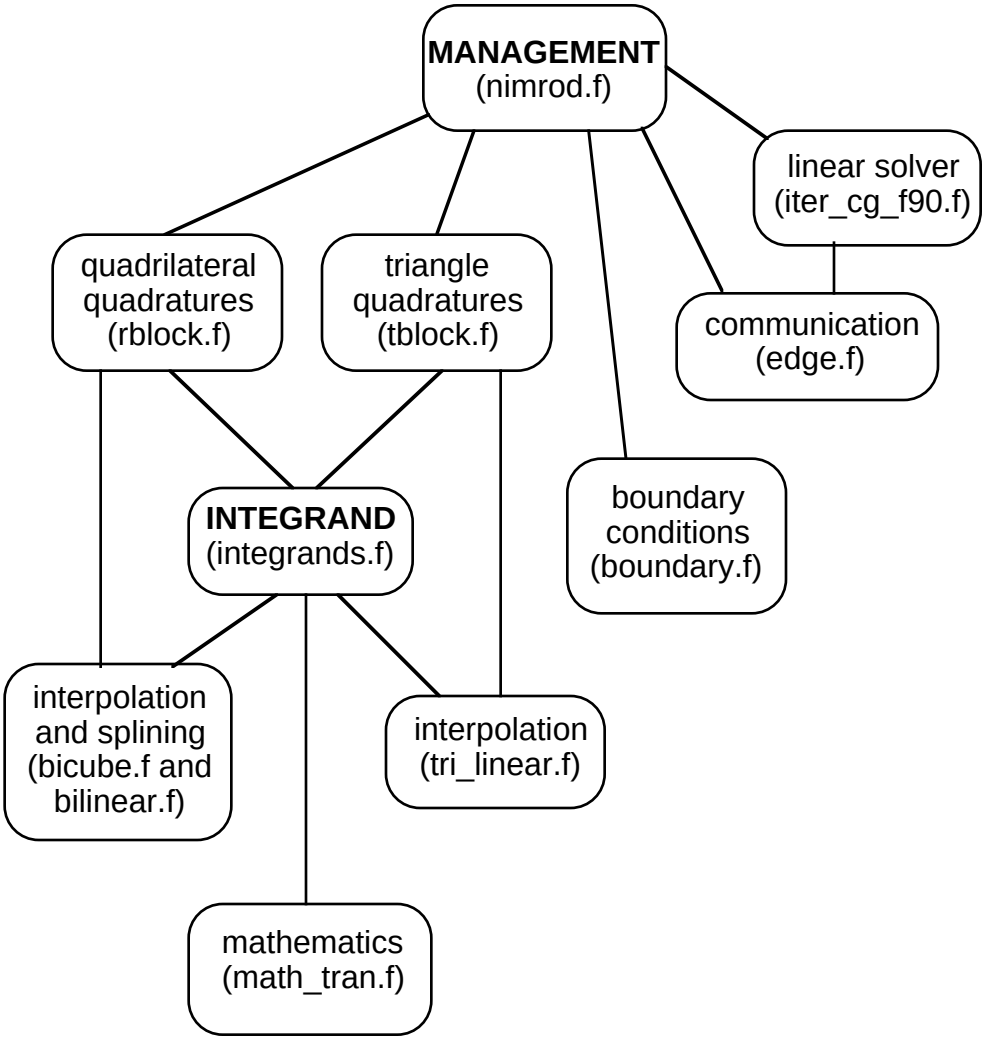

Equation-specific routines are inserted at the **BOLD** levels only, providing flexibility for developers and users.

NIMROD will eventually use an implicit advance for the magnetic field and velocity. It presently uses a semi-implicit formulation.

- The first nonlinear version of NIMROD uses a time-split, semi-implicit algorithm.

  -> Toroidal mode coupling only appears in explicit terms, so matrices are linear in mode number.

  -> Matrices are symmetric, positive definite.

  -> This approach has provided a fast development path to meaningful research computations.

- An implicit algorithm will be more robust and easier to use.

  -> Requires inverting matrices that couple Fourier harmonics.

  -> Will permit accurate computations including the Hall effect at large times steps. [Requires a nonsymmetric matrix solver.]

  -> An existing implicit version has been tested on single toroidal mode MHD waves.

Implicit vs. Semi-implicit formulations (cold plasma only)

Implicit:

$\upsilon = Z_e m_e / m_i$

f_Ω = numerical time-centering parameter

$$\mathbf{E} = \frac{1}{\varepsilon_0 \omega_p^2}\frac{\Delta \mathbf{J}}{\Delta t} + f_\Omega \mathbf{B}^* \times \left(\mathbf{V}^{n+1} - \frac{(1-\upsilon)}{(1+\upsilon)}\frac{1}{en}\mathbf{J}^{n+1} \right)$$

$$+ (1-f_\Omega)\mathbf{B}^* \times \left(\mathbf{V}^{n} - \frac{(1-\upsilon)}{(1+\upsilon)}\frac{1}{en}\mathbf{J}^{n} \right)$$

$$\mathbf{V}^{n+1} = \mathbf{V}^n + \frac{\Delta t}{\rho}\left(f_\Omega \Delta \mathbf{J} + \mathbf{J}^n \right) \times \mathbf{B}^*$$

$$\mathbf{E}_{imp} = \frac{1}{\varepsilon_0 \omega_p^2}\frac{\Delta \mathbf{J}}{\Delta t} + \frac{f_\Omega^2 \Delta t}{\rho}\left(B^{*2}\mathbf{I} - \mathbf{B}^*\mathbf{B}^* \right) \cdot \Delta \mathbf{J} - \frac{(1-\upsilon)}{(1+\upsilon)}\frac{f_\Omega}{en}\mathbf{B}^* \times \Delta \mathbf{J}$$

$$\mathbf{E}_{exp} = \mathbf{B}^* \times \mathbf{V}^n + \frac{f_\Omega \Delta t}{\rho}\left(B^{*2}\mathbf{I} - \mathbf{B}^*\mathbf{B}^* \right) \cdot \mathbf{J}^n - \frac{(1-\upsilon)}{(1+\upsilon)}\frac{1}{en}\mathbf{B}^* \times \mathbf{J}^n$$

$$\Delta \mathbf{B} + \nabla \times \mathbf{Z} \cdot \nabla \times \Delta \mathbf{B} = -\Delta t \nabla \times \mathbf{E}_{exp}$$

$$\mathbf{Z} = \frac{c^2}{\omega_p^2}\mathbf{I} + \frac{f_\Omega^2 \Delta t^2}{\mu_0 \rho}\left(B^{*2}\mathbf{I} - \mathbf{B}^*\mathbf{B}^* \right) - \frac{(1-\upsilon)}{(1+\upsilon)}\frac{f_\Omega \Delta t}{\mu_0 en}\mathbf{B}^* \times \mathbf{I}$$

1. Solve implicit equation for **B**.
2. Advance **V** with time-centered **B**.
3. Iterate for nonlinear convergence.

Semi-implicit:

f_m, f_h are numerical coefficients

$$\mathbf{V}^{n+1} = \mathbf{V}^n + \frac{\Delta t}{\rho}\mathbf{J}^n \times \mathbf{B}^n$$

$$\mathbf{Z}_m = \frac{c^2}{\omega_p^2}\mathbf{I} + \frac{f_m \Delta t^2}{\mu_0 \rho}\left(B_0{}^2\mathbf{I} - \mathbf{B}_0\mathbf{B}_0\right)$$

$$\mathbf{E}_m = \mathbf{B} \times \mathbf{V}^{n+1}$$

$$\mathbf{Z}_h = \frac{(1-\upsilon)}{(1+\upsilon)}\frac{f_h \Delta t}{\mu_0 e n}|\mathbf{B}_0|\,\mathbf{I}$$

$$\mathbf{E}_h = \frac{(1-\upsilon)}{(1+\upsilon)}\frac{1}{en}\mathbf{B}^{**} \times \mathbf{J}^{**}$$

$$\Delta\mathbf{B} + \nabla \times \mathbf{Z}_{m,h} \cdot \nabla \times \Delta\mathbf{B} = -\Delta t \nabla \times \mathbf{E}_{m,h}$$

1. Advance **V** with old **J** and **B**.
2. Solve the matrix equation for $\Delta\mathbf{B}$ using $\mathbf{Z}_m$ and $\mathbf{E}_m$.
3. Solve the matrix equation for $\Delta\mathbf{B}$ using $\mathbf{Z}_h$ and $\mathbf{E}_h$ with $\Delta t \rightarrow \Delta t/2$.
4. Repeat 3. with predicted **J** and the full Δt, completing the Hall split.

In both the implicit and semi-implicit formulations, the shear Alfven wave factors from the compressional wave in the numerical dispersion relation.

Abbreviation of analysis for the implicit formulation:

[see Glasser, “Numerical Analysis of the NIMROD Formulation,” poster 1C26, 1997 Annual Sherwood Fusion Theory Conference for details—available from http://wwwofe.er.doe.gov/More_HTML/NIMROD.HTML]

Assume an $e^{i\mathbf{k}\cdot\mathbf{x}}$ dependence.

$\mathbf{B}_0$ uniform in the $\hat{\mathbf{b}}$ direction.

$\lambda \equiv$ time – step eigenvalue

$\mathbf{Z} \equiv$ effective impedance tensor

Temporal discretization only:

$$(\lambda - 1)\mathbf{B} + \nabla \times (\mathbf{Z} \cdot \nabla \times \mathbf{B}) = 0$$

$$\mathbf{D} \cdot \hat{\mathbf{b}} = 0,\ \mathbf{D} \equiv (\lambda - 1)\mathbf{I} - \mathbf{k} \times (\mathbf{Z} \cdot \mathbf{k} \times \mathbf{I})$$

$$D \equiv \det \mathbf{D} \approx (\lambda - 1)\left[(\lambda - 1) + Z_\perp k_\parallel^2\right]\left[(\lambda - 1) + Z_\perp k_\perp^2\right]$$

Include 2D finite element discretization:

$$\mathbf{K} \equiv -\frac{\sum_j \exp\left[i\mathbf{k}\cdot\left(\mathbf{x}_j-\mathbf{x}_i\right)\right]\int \nabla\alpha_i\nabla\alpha_j d\mathbf{x}}{\sum_j \exp\left[i\mathbf{k}\cdot\left(\mathbf{x}_j-\mathbf{x}_i\right)\right]\int \alpha_i\alpha_j d\mathbf{x}},$$

where α_j is the bilinear basis element centered at vertex j.

$$D \approx \left[(\lambda-1)+Z_\perp\left(\hat{\mathbf{b}}\hat{\mathbf{b}}:\mathbf{K}\right)\right]\times$$
$$\left\{\begin{array}{l}(\lambda-1)\left[(\lambda-1)+Z_\perp\,\mathrm{tr}\left(\mathbf{K}\right)\right]+\\ Z_\perp^2\left[\left(\hat{\mathbf{b}}\hat{\mathbf{b}}:\mathbf{K}\right)\mathbf{K}:\left(\mathbf{I}-\hat{\mathbf{b}}\hat{\mathbf{b}}\right)-\hat{\mathbf{b}}\cdot\mathbf{K}\cdot\left(\mathbf{I}-\hat{\mathbf{b}}\hat{\mathbf{b}}\right)\cdot\mathbf{K}\cdot\hat{\mathbf{b}}\right]\end{array}\right\}$$

- The last line represents truncation error that couples the zero-frequency mode with the compressional branch. This has not produced any observable effects in the simulations completed to date.

- That the shear branch factors from the compressional branch implies that the formulation effectively treats the stiffness of the MHD equations. Validation results confirm this conclusion.

Linear Solver

NIMROD's performance, hence its ability to solve 'cutting edge' physics problems, depends critically on the linear solver used to invert matrices.

- Equations have been formulated so that matrices are symmetric, positive definite (so far).

- We presently use a preconditioned conjugate gradient technique.

  -> guaranteed convergence
  -> minimal memory requirements
  -> basic iteration scheme involves matrix/vector products, so parallel computing is not a problem

- Existing preconditioner options:

  -> basic diagonal 'point block' inversion
  -> grid-block direct inversion ('additive Schwartz')
  -> incomplete factorization
  -> 1D direct solves

- Other possibilities for preconditioning:

  -> linking to packaged routines such as ISIS and AZTEC
  -> multigrid

- We plan to implement a solver for nonsymmetric matrices (GMRES?) to enhance numerical flexibility.

Preprocessing

- FLUXGRID:

-> Reads the output from an equilibrium code (either direct or inverse solve).
-> Or reads an equilibrium and eigenfunction (as an initial perturbation) from GATO.
-> Generates a grid based on equilibrium flux surfaces.

- NIMSET:

-> Reads a FLUXGRID data file.
-> Decomposes the grid into blocks.
-> Generates block connections and vertex connections within blocks of unstructured triangles.
-> Generates an initial perturbation.
-> Writes the initial NIMROD dump file.

Postprocessing

- NIMPLOT:

-> Reads NIMROD dump files.
-> Generates binary data files for XDRAW graphics.
-> Creates Poincare surfaces of section data.
-> We plan to have an option for generating DX data files (presently being done from NIMROD directly).

- XDRAW:

-> Publicly available
-> Grid plots
-> Spatial slices
-> Slices showing temporal dependence
-> Time-history traces
-> Contour plots over the poloidal plane (by Fourier mode or at a specified toroidal angle)
*See Poincare movie demonstration.

- IBM Data Explorer:

-> Multi-dimensional movies
-> Sophisticated, 3D data rendering available

Validation Program

Shear Alfven Wave Tests

- Uniform rectangular grid, doubly periodic, 1m on a side.
- Neither **k** nor **B** are aligned with the grid ($k_x=k_y=2\pi$, $k_z=2^{3/2}\pi$).
- $k_{\|}/k = 2.5\%$
- The two traces for each formulation are for an 8x8 grid [larger error] and for a 16x16 grid.

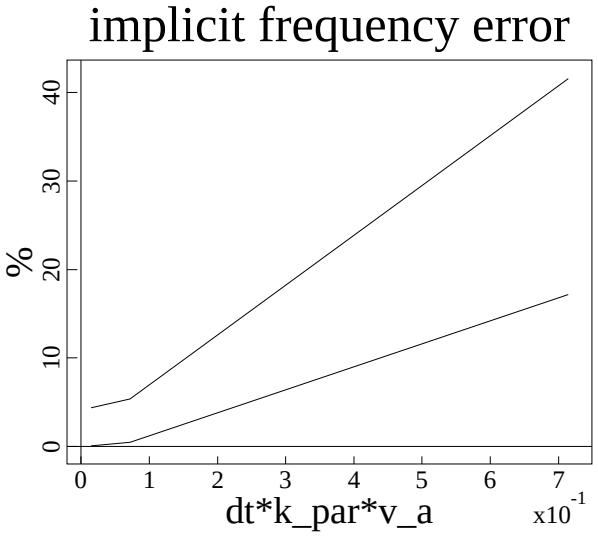

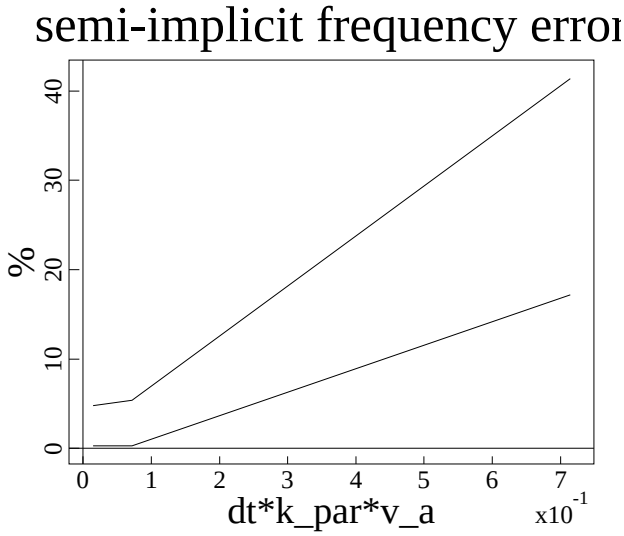

The largest time-step cases for the 16x16 grids have $v_A \Delta t/\Delta x = 37$. The strong spatial convergence verifies the decoupling of shear and compressional waves in the numerical dispersion relations.

Our semi-implicit formulation shows no loss of accuracy with respect to the implicit formulation.

Magneto-acoustic Waves

- Uniform rectangular grid, periodic in y, 1m on a side.
- $k_y=2\pi$
- $\omega^2 = \omega_A^2\left(1+\frac{\gamma\beta}{2}\right), \qquad \gamma = \frac{5}{3}$

$\beta = 2\mu_0 P_0 / B_0^2$	MA CFL	cells	$1+\gamma\beta/2$	$(\omega/\omega_A)^2$
1	2.2	16	1.833	1.684
1	1.1	16	1.833	1.843
1	0.54	16	1.833	1.836
1	1.1	32	1.833	1.831
1/2	1.9	16	1.417	1.308
1/2	0.95	16	1.417	1.416

Whistler Waves

- Hall-only in Ohm's law (low frequency limit).

$$\det\left[\omega_w^2\mathbf{I} - \frac{(\mathbf{k}\cdot\mathbf{B}_0)^2}{\mu_0^2 e^2 n^2}\left(k^2\mathbf{I} - \mathbf{kk}\right)\right] = 0$$

- **k** || $\mathbf{B}_0$, k=2π , **z** is Fourier, **y** is finite element.

k	$\omega_w\Delta t$	cells	ω/ω_w	ω_i/ω_w
z	0.314		0.75	-0.013
z	0.157		0.86	-0.0046
z	0.0785		0.93	-0.0014
y	0.314	8	0.73	-0.013
y	0.157	8	0.85	-0.0046
y	0.157	16	0.86	-0.0044

Ideal MHD Instabilities

Soloviev Ideal Internal Mode
(Courtesy of Dalton Schnack)

R=3m, a=1m, q_0=0.4, elongation=1

n=2 mode (Berger, et al. find a growth rate of $2.56X10^5$)

dissipation[1]	grid	Δt	growth rate[2]
1000	32x32	$2.5X10^{-8}$	$2.06X10^5$
100	32x32	$2.5X10^{-8}$	$2.30X10^5$
10	32x32	$2.5X10^{-8}$	$2.36X10^5$
0	32x32	$2.5X10^{-8}$	$2.36X10^5$
0	32x32	$1.3X10^{-8}$	$2.40X10^5$
1000	64x64	$2.5X10^{-8}$	$2.05X10^5$
0	64x64	$2.5X10^{-8}$	$2.40X10^5$

[1]Electrical diffusivity and kinetic viscosity.

D3D Ideal Internal Kink Modes

n=1 growth rate comparison* with GATO calculations:

dissipation[1]	grid[2]	β_N=0	β_N=1	β_N=2
GATO	100x200	stable	0.038	0.087
S=1.6X10^4	65x31	0.030	0.055	0.092
S=1.6X10^5	65x63	insuf. grid	0.043	0.081
same ν, but η=0	65x31	stable	0.032	0.077

[1]NIMROD simulations have resistivity, viscosity, and no-slip boundary conditions. GATO is ideal and uses free-slip boundary conditions

[2]The NIMROD grid is uniform in the flux surface-normal direction in these cases, while the GATO grid is packed at low-order rational surfaces.

*The NIMROD results are not fully converged.

Convergence study for S=1.6X10^4, β_N=2 case:

grid	Δt	dissipation centering	semi-imp coefficient	growth rate
65x31	2X10^{-8}	1	1.5	0.0865
65x31	1X10^{-8}	1	1.5	0.0916
65x31	5X10^{-9}	1	1.5	0.0925
65x31	1X10^{-8}	1/2	1.0	0.0921
25x23	1X10^{-8}	1	1.5	0.101
33x31	1X10^{-8}	1	1.5	0.0916
49x47	1X10^{-8}	1	1.5	0.0866

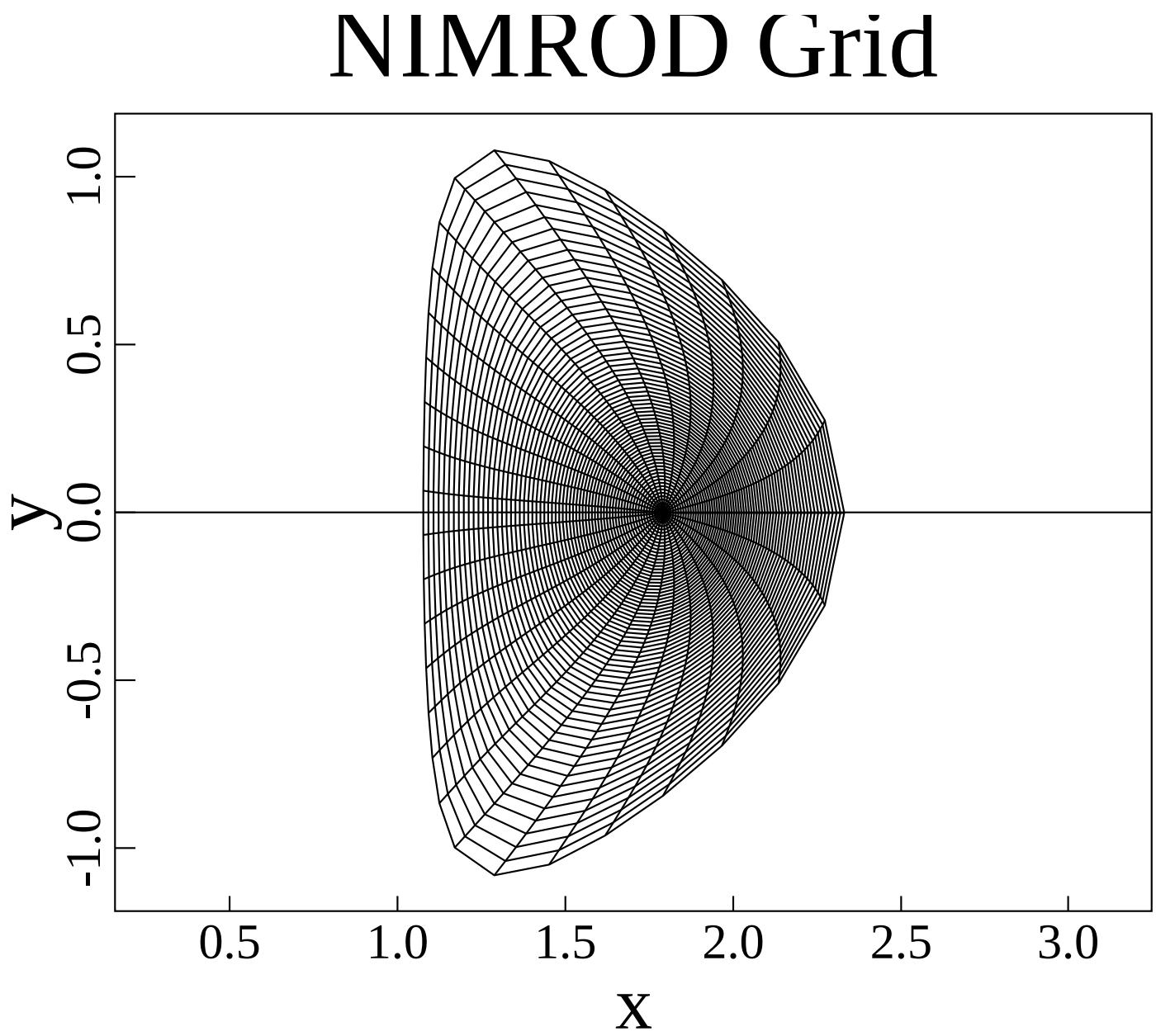
NIMROD Grid
y
1.0
0.5
0.0
-0.5
-1.0
0.5
1.0
1.5
2.0
2.5
3.0
x

Linear Eigenfunction Comparison for the β_N=1 Case

GATO NIMROD

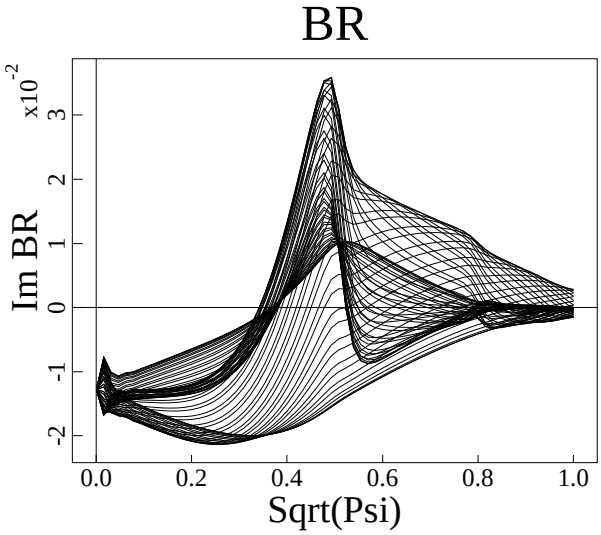
BR
Im BR
x10^-2
3
2
1
0
-1
-2
0.0
0.2
0.4
0.6
0.8
1.0
Sqrt(Psi)

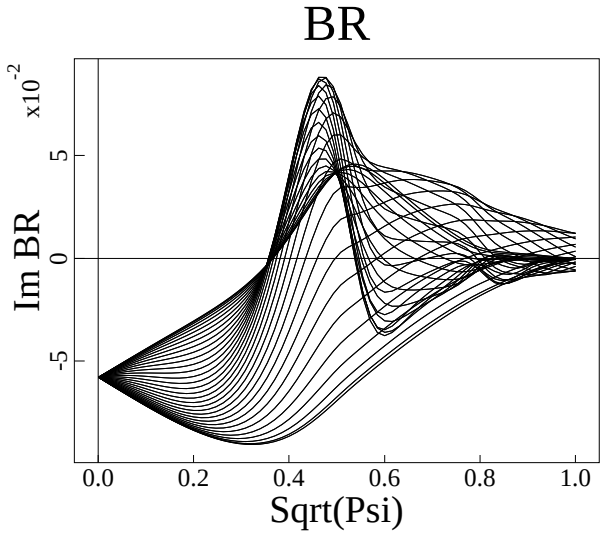
BR
Im BR
x10^-2
5
0
-5
0.0
0.2
0.4
0.6
0.8
1.0
Sqrt(Psi)

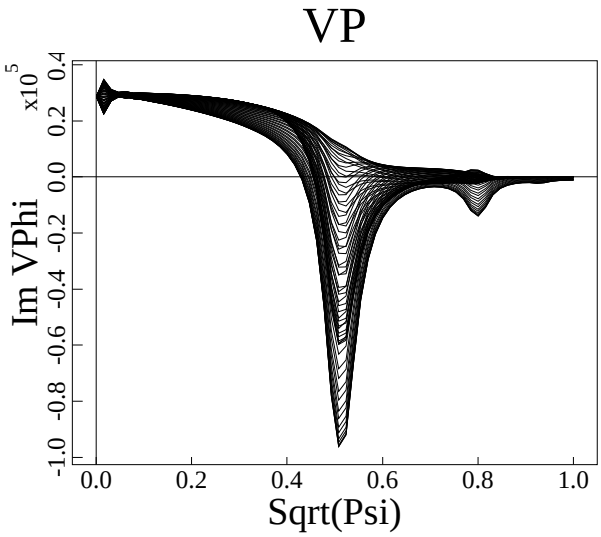
VP
Im VPhi
x10^5
0.4
0.2
0.0
-0.2
-0.4
-0.6
-0.8
-1.0
0.0
0.2
0.4
0.6
0.8
1.0
Sqrt(Psi)

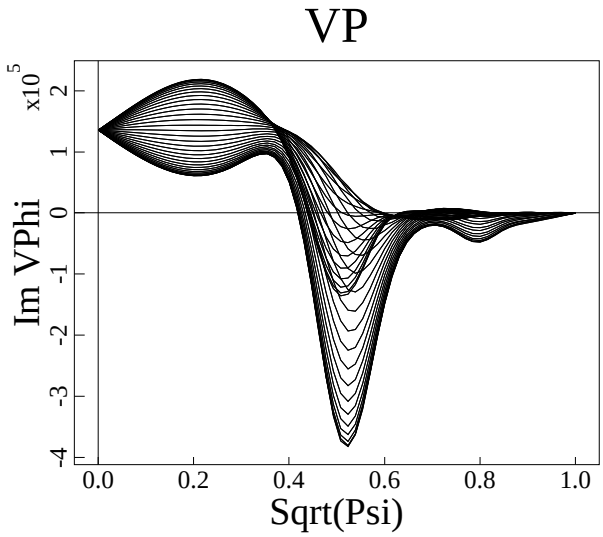
VP
Im VPhi
x10^5
2
1
0
-1
-2
-3
-4
0.0
0.2
0.4
0.6
0.8
1.0
Sqrt(Psi)

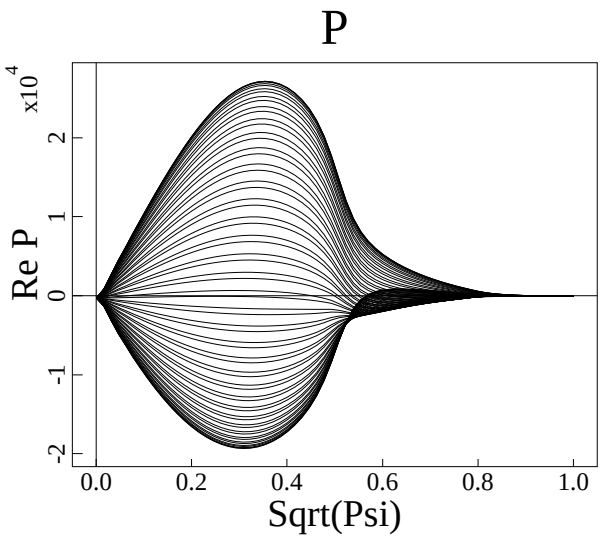
P
Re P
x10^4
2
1
0
-1
-2
0.0
0.2
0.4
0.6
0.8
1.0
Sqrt(Psi)

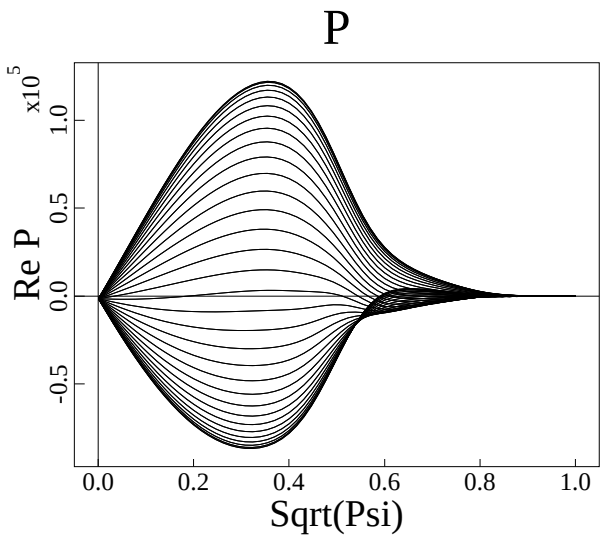
P
Re P
x10^5
1.0
0.5
0.0
-0.5
0.0
0.2
0.4
0.6
0.8
1.0
Sqrt(Psi)

Nonlinear Saturation of the β_N=2, D3D Ideal Internal Kink with S decreased to 1.6X10^3
(larger S will require more spatial resolution)

*The advection term is not included in the momentum equation.

[Also see the Poincare surface of section movie.]

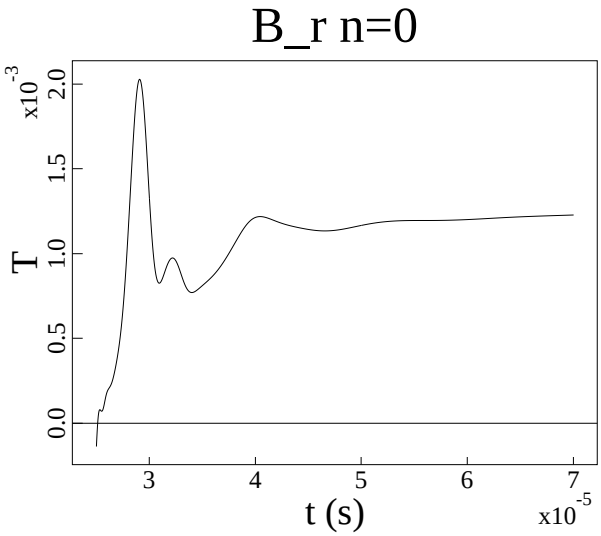

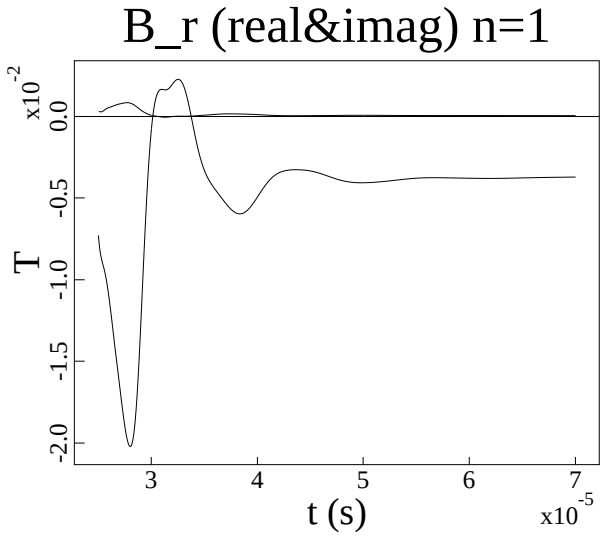

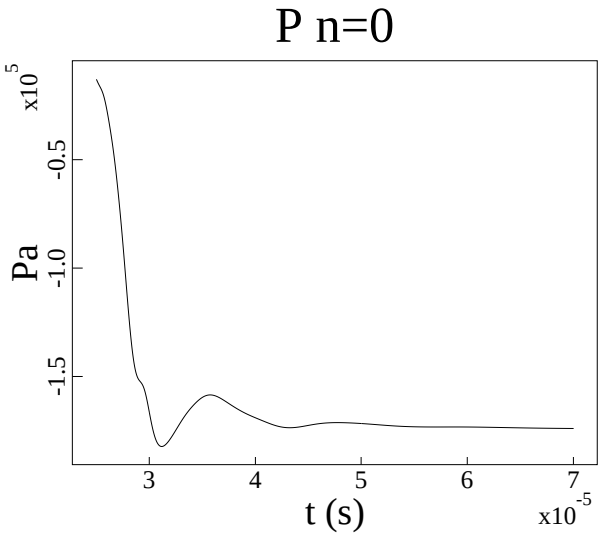

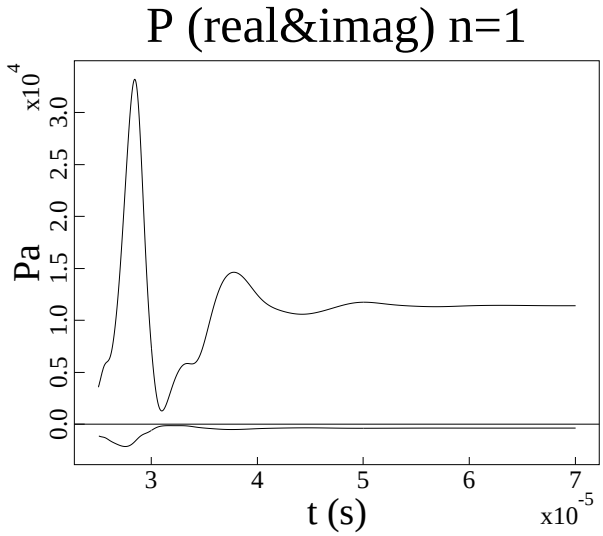

Linear Resistive MHD Instability

- External mode in a linear periodic cylinder with a conducting shell at the plasma surface.
- 0-β, paramagnetic equilibrium (flow removed)
- Normalized current density on axis is 3.5. Robinson found marginal resistive stability at 2.5 and marginal ideal stability at 4.1 for m=1, k=-0.6 (no viscosity). [D. C. Robinson, Nuclear Fusion **18**, 939 (1978)]
- First convergence study performed at S=1000 and P_m=1.
- DEBS converges on $\gamma\tau_A$=0.028
- NIMROD:

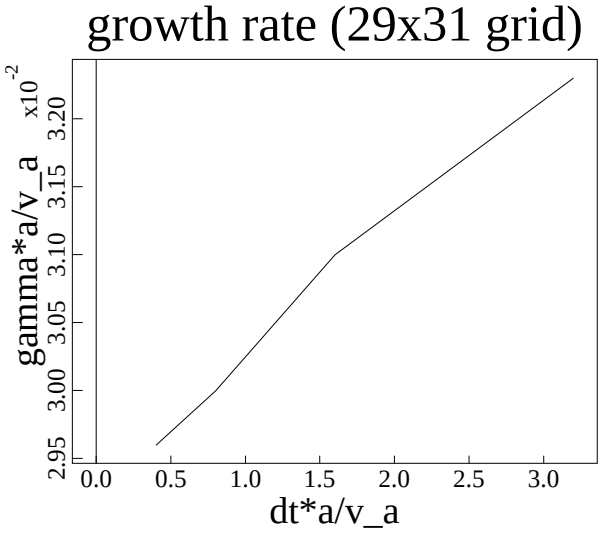

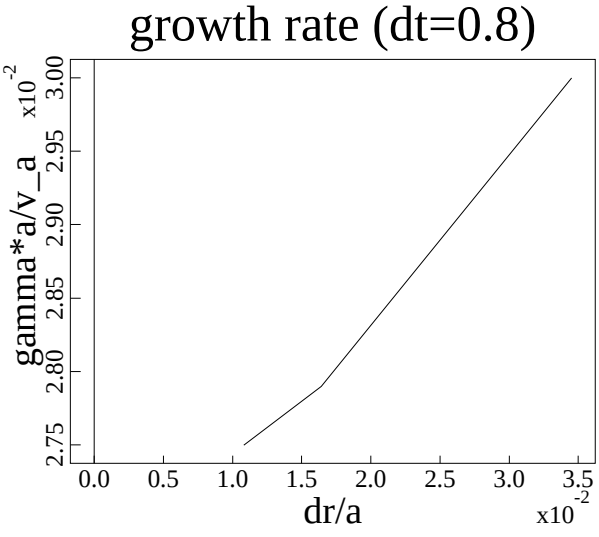

Eigenfunction Comparison (B_r) for a Tearing Mode in a Periodic Cylinder

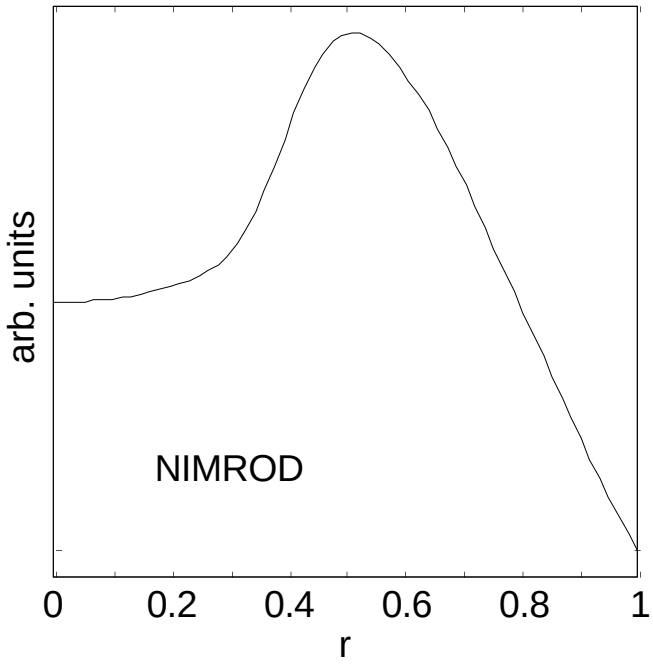

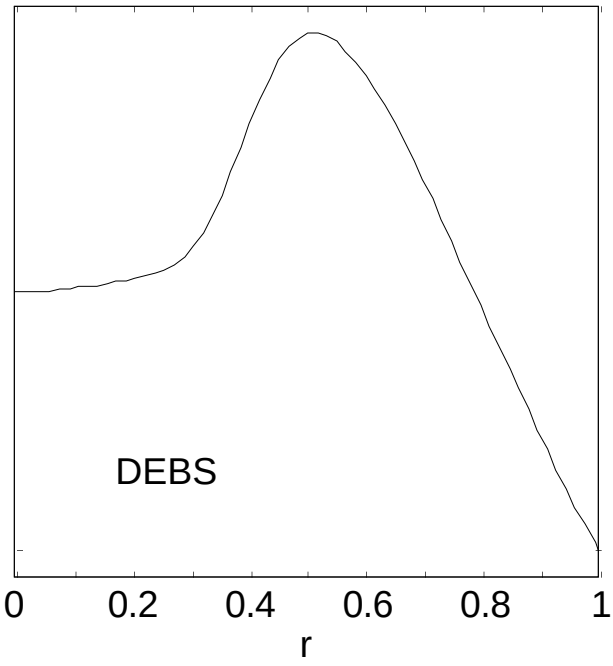

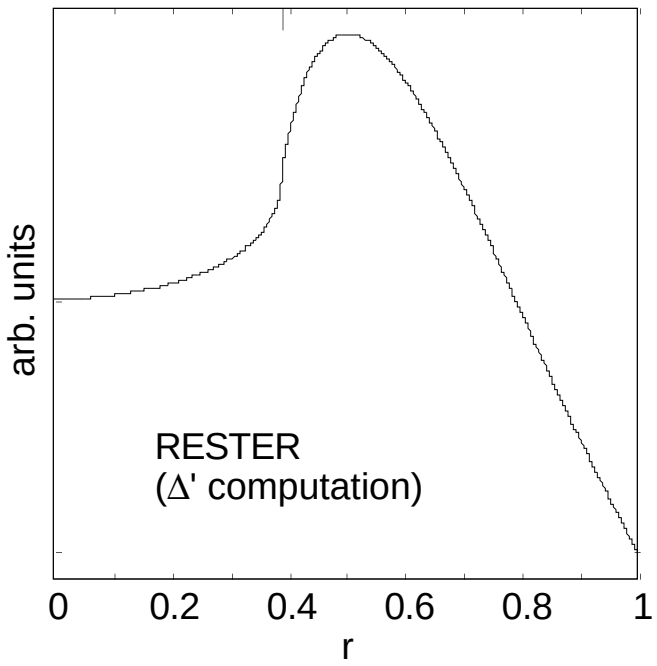

1. No viscosity
2. S=1000 for NIMROD and DEBS
3. Paramagnetic Equilibrium
4. m=1, k=-0.60
5. A convergence study for growth rates is in progress, $\gamma\tau_A$~0.01.
6. Normalized J(0)=3.0

Nonlinear Saturation of the Resistive Mode

- Same parameters as the J(0)=3.5 linear case, except the pinch flow is retained.
- Advection is included in the momentum equation.
- Computed with the k=0 and k=0.6 Fourier modes only.
- 29x31 grid and $\Delta t=0.4\ \tau_A$ in NIMROD
- DEBS n=1, B_r saturation amplitude is 0.031 (same radial mesh, $\Delta t=0.1\ \tau_A$, no convergence check)

Magnetic Energy (n=1)

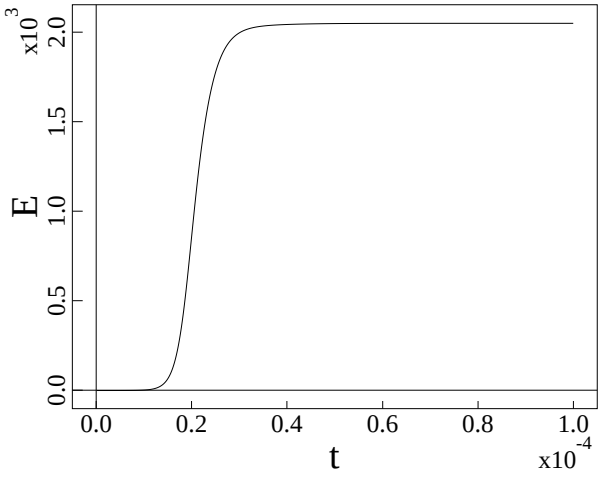

Kinetic Energy (n=1)

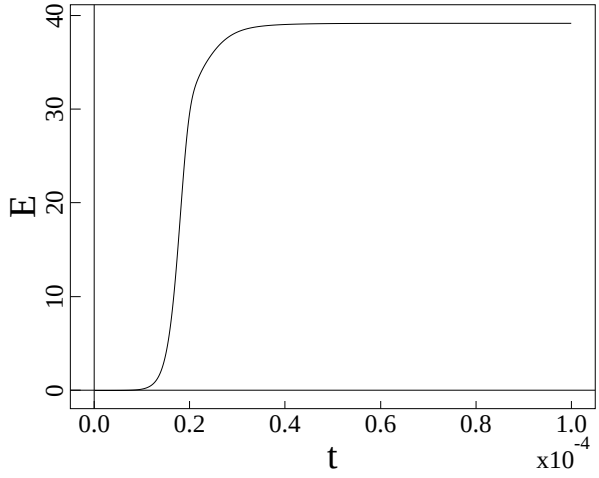

Saturated Br (n=1)

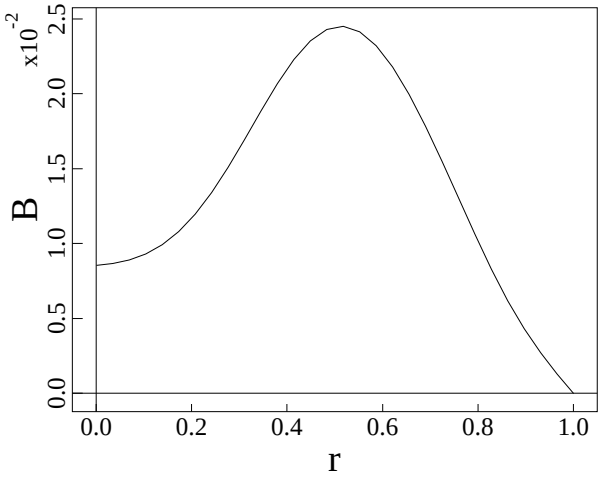

Saturated Vr (n=1)

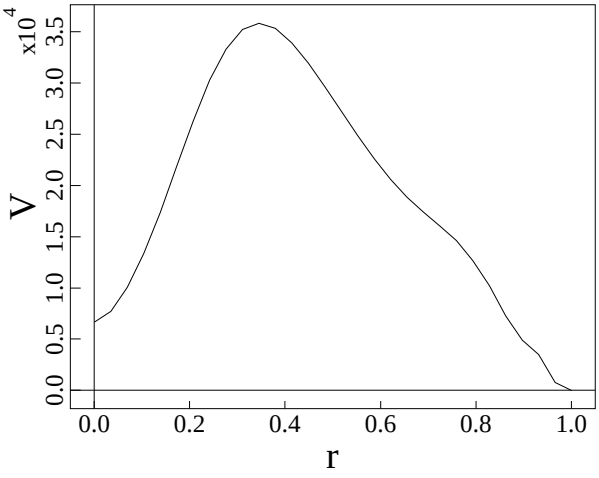

Quasilinear Effects

before

J.B/B**2

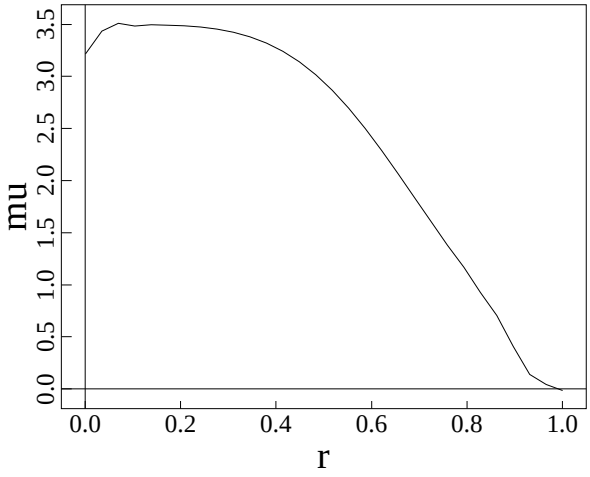

safety factor

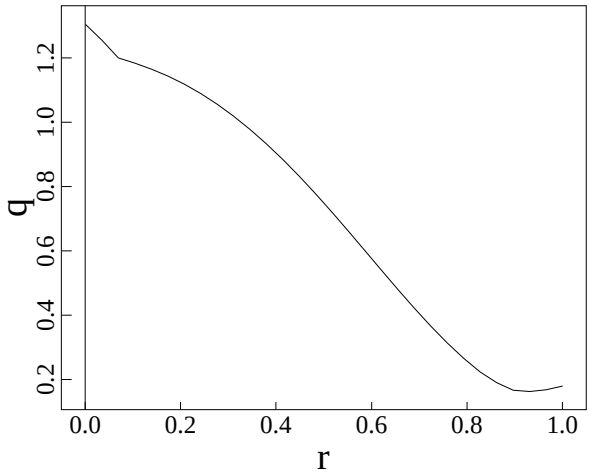

after

J.B/B**2

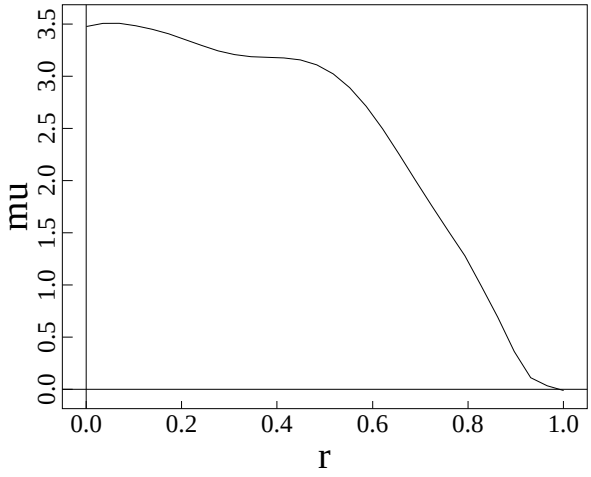

safety factor

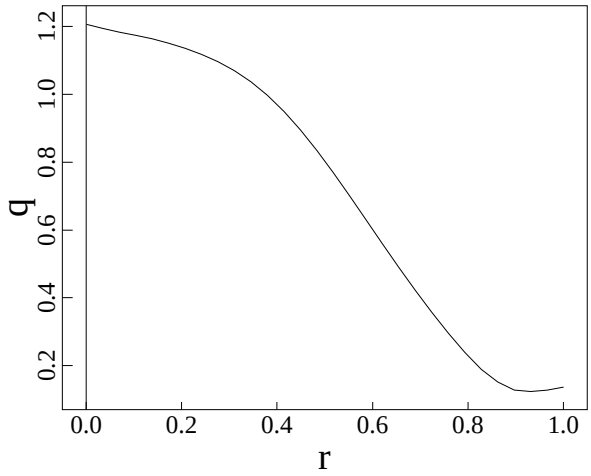

Note: problems near the magnetic axis result from the computation of J, which are used for the diagnostics only.

Plans for Completing the First Production Version

1. Presently the code can only apply boundary conditions to blocks of rectangles. We need to add boundary routines for the blocks of triangles. This is essential, because the triangles will be used for gridding complex experimental wall structures.

2. We intend to keep the source code in Concurrent Versions System (CVS) format to reduce the burden of code development by multiple users.

Intermediate-term plans

1. Complete the validation plan.

2. Begin research simulations: a simulation of an RFP in toroidal geometry is underway.

3. Improve the linear-solver preconditioner for shorter execution times.

4. Implement a ‘vacuum’ region mock-up via a highly diffusive region that moves with the plasma surface. This will allow nonlinear simulations of external modes in tokamaks.

5. Implement R=0 boundary conditions for spheromak simulations.

6. Finish coding the complete implicit formulation.

Summary

- The effort spent developing a good numerical formulation is paying dividends in the form of rapid benchmarking progress.
- Primary features of NIMROD include flexibility regarding the terms used in the fluid equations and in the geometry of the problem domain.
- NIMROD has been developed with modular programming and user-interface features to make the code user-friendly.
- NIMROD is essentially ready for attacking research problems.

Don’t sign-up, net-up!

This poster will be available from

http://wwwofe.er.doe.gov/More_HTML/NIMROD.HTML

along with presentations from previous meetings.